Learning-related feedforward inhibitory connectivity growth required for memory precision.

UNIVERSITÀ DEGLI STUDI DI TORINO

Nature 473 (7348) 2011 : 514–518

DOI : 10.1038/nature09946

LEARNING-RELATED FEEDFORWARD INHIBITORY CONNECTIVITY GROWTH REQUIRED FOR MEMORY PRECISION

Sarah Ruediger[1*], Claudia Vittori[1,2*], Ewa Bednarek[1], Christel Genoud[1], Piergiorgio Strata[2], Benedetto Sacchetti[2] & Pico Caroni[1]

[1]Friedrich Miescher Institute, Maulbeerstrasse 66, CH-4058 Basel, Switzerland.
[2]Department of Neuroscience and National Institute of Neuroscience-Italy, C.so Raffaello 30, 10125 Torino, Italy.

*These authors contributed equally to this work.

In the adult brain, new synapses are formed and pre-existing ones are lost, but the function of this structural plasticity has remained unclear[1,2,3,4,5]. Learning of new skills is correlated with formation of new synapses[6,7,8]. These may directly encode new memories, but they may also have more general roles in memory encoding and retrieval processes[2]. Here we investigated how mossy fibre terminal complexes at the entry of hippocampal and cerebellar circuits rearrange upon learning in mice, and what is the functional role of the rearrangements. We show that one-trial and incremental learning lead to robust, circuit-specific, long-lasting and reversible increases in the numbers of filopodial synapses onto fast-spiking interneurons that trigger feedforward inhibition. The increase in feedforward inhibition connectivity involved a majority of the presynaptic terminals, restricted the numbers of c-Fos-expressing postsynaptic neurons at memory retrieval, and correlated temporally with the quality of the memory. We then show that for contextual fear conditioning and Morris water maze learning, increased feedforward inhibition connectivity by hippocampal mossy fibres has a critical role for the precision of the memory and the learned behaviour. In the absence of mossy fibre long-term potentiation in *Rab3a*$^{-/-}$ mice[9], c-Fos ensemble reorganization and feedforward inhibition growth were both absent in CA3 upon learning, and the memory was imprecise. By contrast, in the absence of adducin 2 (Add2; also known as β-adducin)[10] c-Fos reorganization was normal, but feedforward inhibition growth was abolished. In parallel, c-Fos ensembles in CA3 were greatly enlarged, and the memory was imprecise. Feedforward inhibition growth and memory precision were both rescued by re-expression of Add2 specifically in hippocampal mossy fibres. These results establish a causal relationship between learning-related increases in the numbers of defined synapses and the precision of learning and memory in the adult. The results further relate plasticity and feedforward inhibition growth at hippocampal mossy fibres to the precision of hippocampus-dependent memories.

Subject terms: Neuroscience - Cell biology - Animal behaviour - Molecular biology

MAIN

To determine whether hippocampus-dependent learning[11,12,13] may produce structural rearrangements in hippocampal large mossy fibre terminal (LMT) components involved in feedforward excitation and/or feedforward inhibition in CA3 (ref. 14) (Fig. 1a and Supplementary Material), we analysed GFP-positive LMTs in the dorsal hippocampus of *Thy1-mGFP(Lsi1)* reporter mice[5] that had been subjected to contextual fear conditioning, a one-trial learning protocol (Methods). Fear conditioning led to a robust increase in the average number of filopodia per LMT (1.82-fold, $P < 0.001$; feedforward inhibition connectivity; Fig. 1b, c and Supplementary Fig. 2a), and to a less pronounced increase in the average numbers of Bassoon-positive putative release sites per core LMT[15] (1.31-fold, $P < 0.01$; feedforward excitation connectivity; Supplementary Fig. 2a). By contrast, there was no change in the densities of LMTs in CA3b at any time upon fear conditioning (Supplementary Fig. 2a). The filopodia contacted spine-free dendrites of parvalbumin-positive interneurons in CA3b (Fig. 1d, e and Supplementary Fig. 3a), indicating that they induce feedforward inhibition through fast-spiking interneurons[16,17,18]. To estimate the fraction of LMTs in CA3b with altered contents of filopodia, we analysed LMT/filopodia distributions in naive, control and fear-conditioned mice. Shifts in the fractions of LMTs with no filopodia and with more than four filopodia revealed that, on average, at least 45% of the LMTs established increased numbers of filopodia as a consequence of fear conditioning (Fig. 1f).

To determine whether an increase in stratum lucidum feedforward inhibition connectivity may be generally associated with hippocampal learning, we analysed mice that underwent a Morris water maze incremental learning protocol. Filopodial contents were only slightly increased over naive values during the first 3–4 days of training, whereas they increased markedly between days 4 and 8 (Fig. 1g). Again, we detected no changes in the densities of LMTs in CA3b upon Morris water maze learning (not shown). Testing mice for the memory of the platform position revealed that this reference memory only began to differ from chance after 3 days of training (Fig. 1h). The reference memory reached plateau values at day 8 (Fig. 1h), suggesting that filopodial growth correlated with the establishment of a precise spatial memory in the Morris water maze test. The reference memory of the platform position persisted for at least 45 days after cessation of the training and, unlike in the fear conditioning experiment, raised filopodia per LMT values also persisted for at least 45 days (Fig. 1h; day 53 values). As in the fear conditioning experiment, a large fraction of the LMTs exhibited higher filopodial contents at plateau values (Fig. 1i).

Figure 1: Learning-related feedforward inhibition connectivity growth in the hippocampus.

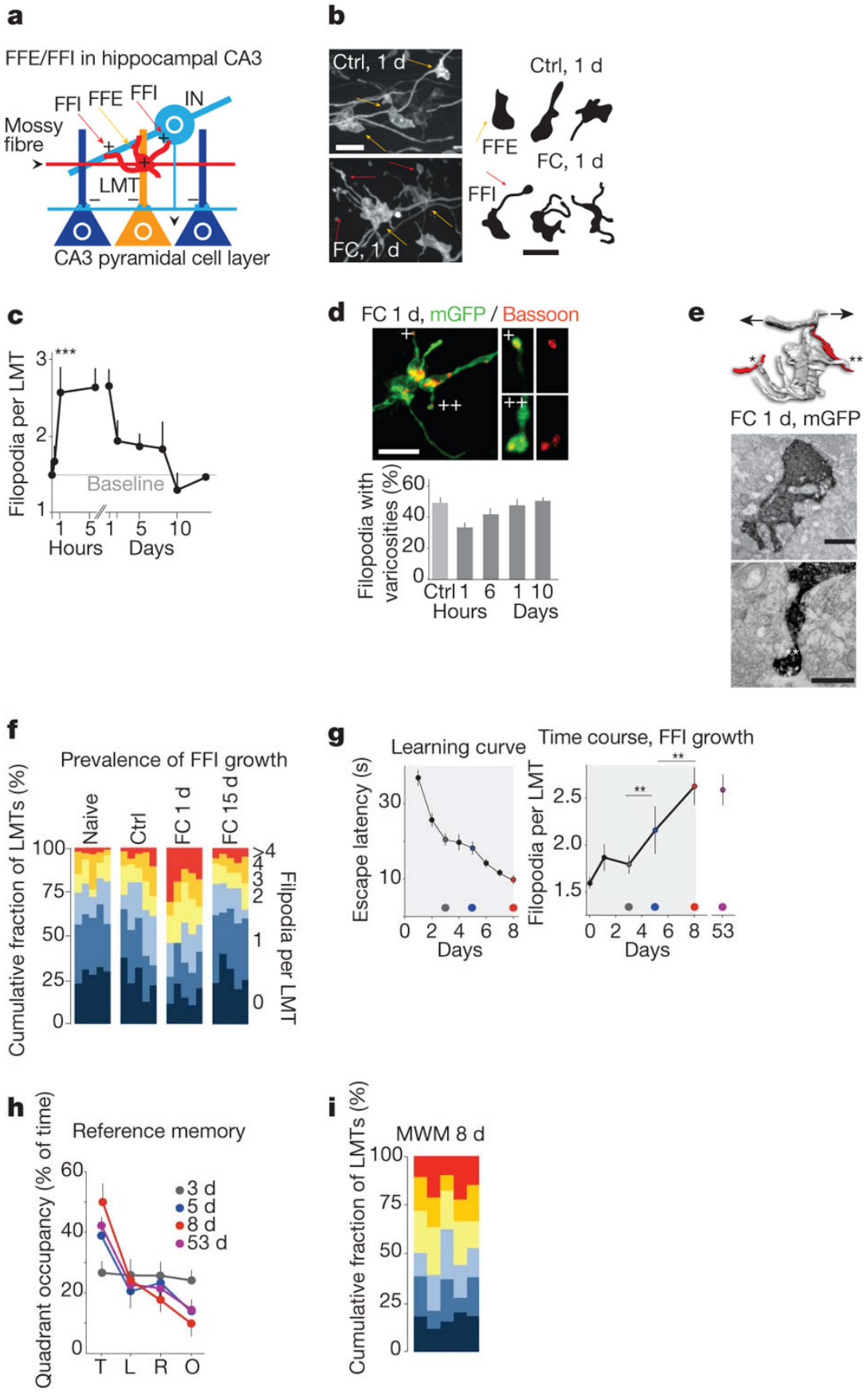

a, Schematic of hippocampal feedforward excitation (FFE) and feedforward inhibition (FFI) circuit in stratum lucidum of CA3. IN, inhibitory interneuron. **b**–**f**, Feedforward inhibition growth at hippocampal mossy fibre LMTs upon contextual fear conditioning. **b**, Micrographs and representative camera lucidas of mGFP-labelled mossy fibres and LMTs in hippocampal stratum lucidum (CA3b). Yellow arrows, core LMTs; red arrows, filopodia. Ctrl; control; FC, fear conditioning. **c**, Average filopodia/LMT values upon fear conditioning. $N = 5$ mice (100 LMTs each). $^{***}P < 0.001$. **d**, Filopodial synapses upon fear conditioning. Overview panel shows maximal intensity projection of mGFP-positive LMT with four filopodia. Detail panels show single confocal planes of two of the filopodia (+ and ++); Bassoon channel masked using three-dimensional isosurface of GFP-positive LMT. Bar diagram shows fraction of LMT filopodia with varicosities as a function of time upon fear conditioning ($N = 3$, 100 LMTs). **e**, Filopodia upon fear conditioning learning contact spine-free dendrites. Immuno-electron microscopy of mGFP-positive LMT with four filopodia, 1 day after fear conditioning. Top, three-dimensional reconstruction of immuno-labelled LMT (red, spine-free dendrites contacted by two of the filopodia in the example (marked by one and two asterisks, respectively). Centre, immuno-labelled LMT. Bottom, filopodium with contact is marked by two asterisks. **f**, Distributions of filopodia per LMT contents for individual mice. $N = 100$ LMTs. Relative contents of LMTs with 0, 1, 2, 3, 4, >4 filopodia as a fraction of the total LMT population. Vertical rows, individual mice. **g**–**i**, Feedforward inhition growth at hippocampal mossy fibre LMTs upon Morris water maze (MWM) training. **g**, Learning curve and time course of feedforward inhibition growth. $N = 5$ mice (100 LMTs each). Grey area shows daily training period. The circles highlight the positions on the curves as compared to reference memory (right). **h**, Reference memory at 3, 5, 8 and 53 days. Percentage of time spent by the mice in target (T), left (L), right (C) and opposite (O) quadrants. $N = 5$ mice. **i**, Filopodia per LMT distributions after 8 days of training, as described in **b**. Scale bars, 5 μm (**b**, **d**, top and **g**), 1 μm (**d**, bottom centre) and 0.5 μm (**d**, bottom right).

To determine whether learning-related induction of feedforward inhibition connectivity growth might be a general phenomenon not restricted to spatial learning in the hippocampus, we analysed mossy fibre terminals in the cerebellar cortex, which also consist of powerful large core structures associated with filopodia[19]. Cued fear conditioning, in which animals learn that a tone predicts an aversive stimulus, involves plasticity in cerebellar cortex lobule 5, but not lobule 9 (ref. 20). In parallel, cued fear conditioning led to a robust and reversible increase of filopodial numbers per mossy fibre terminal in lobule 5, but not lobule 9 (Fig. 2a, d). In a second set of experiments, we trained mice to balance on an accelerating rotating rod (rotarod). This cerebellum-dependent motor skill task involved incremental learning over 4–6 days, which was accompanied by a parallel increase in the filopodial contents of mossy fibre terminals in lobule 9, but not lobule 5 (Fig. 2b, d). At least for the Golgi cells that could be visualized with the marker RC3, mossy fibre terminal filopodia extended along their dendrites, and established numerous varicosities, where synaptic markers co-distributed (Fig. 2c and Supplementary Fig. 4). More than 95% of the filopodial varicosities within a granule cell layer volume exhibiting an RC3-positive Golgi cell made putative synaptic contacts with that Golgi cell. Therefore, learning is specifically correlated with the growth of feedforward inhibition connectivity in both hippocampal and cerebellar circuits.

Figure 2: Specificity of learning-related feedforward inhibition growth.

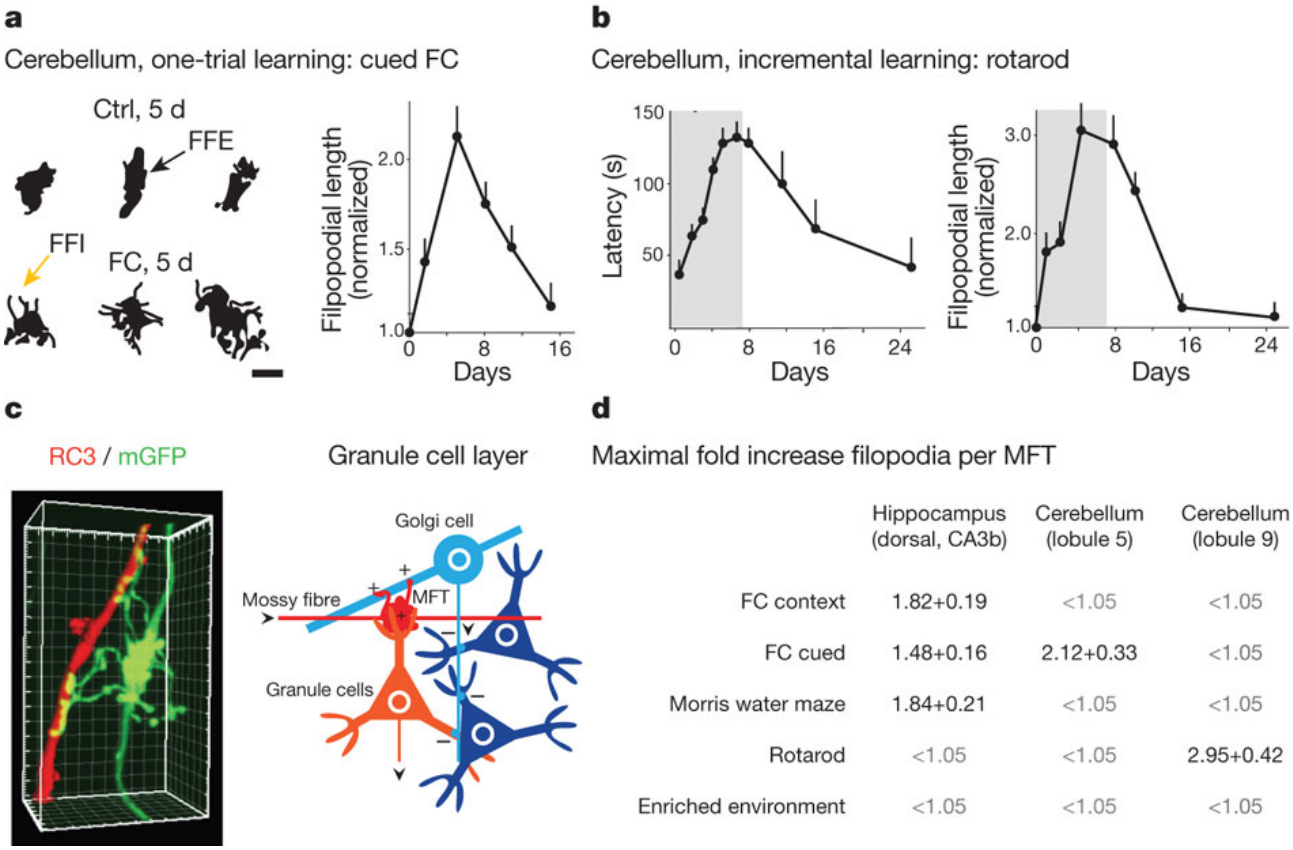

	Hippocampus (dorsal, CA3b)	Cerebellum (lobule 5)	Cerebellum (lobule 9)
FC context	1.82+0.19	<1.05	<1.05
FC cued	1.48+0.16	2.12+0.33	<1.05
Morris water maze	1.84+0.21	<1.05	<1.05
Rotarod	<1.05	<1.05	2.95+0.42
Enriched environment	<1.05	<1.05	<1.05

a, **b**, Learning-related feedforward inhibition connectivity growth in cerebellar cortex. **a**, Feedforward inhibition growth at lobule 5 cerebellar cortex mossy fibre terminals upon cued fear conditioning. Labelling as in **Fig. 1b**. Scale bar, 10 µm. **b**, Feedforward inhibition growth at lobule 9 cerebellar cortex mossy fibre terminals (MFTs) upon rotarod learning. Labelling as in **Fig. 1c**. **c**, In cerebellar cortex, mossy fibre terminal filopodia contact inhibitory Golgi cells. Left, three-dimensional rendering of contacts by mossy fibre terminal filopodia onto RC3-positive Golgi cell dendrite. Right, feedforward excitation/feedforward inhibition circuit in granule cell layer of cerebellar cortex. **d**, Specific relationship between learning and feedforward inhibition growth. Average fold increase values at peak response (fear conditioning hippocampus, 1 day; fear conditioning cerebellum, 2 days; Morris water maze, 8 days; rotarod, 5 days). $N = 5$, 100 LMTs or mossy fibre terminals each.

We next sought to determine what might be the function of the learning-related growth in feedforward inhibition connectivity. In the fear conditioning experiments, the excess filopodia were lost within 8–10 days after learning, and filopodial retention was prolonged upon re-exposure to context leading to extinction (Fig. 3a), indicating that the excess filopodia are not a requirement for expression of the fear memory. Testing of individual mice during the Morris water maze training protocol revealed a strong correlation between the reference memory of the platform position and mean filopodial contents per LMT for individual mice (Fig. 3b), indicating that the extent of filopodial growth was correlated to the precision of the learning. We therefore monitored generalization, that is, decreased behavioural precision of the fear memory in the contextual fear conditioning experiment. In agreement with previous reports[21, 22], generalization of the memory for context in fear conditioning

was not detectable during the first 5–7 days after learning, but was detected at longer intervals after fear conditioning as an enhanced freezing response and reduced exploratory activity in a neutral context (Fig. 3c). A brief re-exposure of mice to training context in the absence of the aversive stimulus at 15 days after learning produced a suppression of generalization at retest, which lasted 8–12 days (Fig. 3d). In parallel, training context re-exposure induced a pronounced re-induction of the filopodial response, which again lasted for 7–10 days (Fig. 3d). By contrast, exposure to a neutral context affected neither generalization nor filopodial growth (Fig. 3d), suggesting that retrieval of the specific memory was necessary to re-induce feedforward inhibition connectivity growth in hippocampal CA3, and to suppress generalization.

Figure 3: Correlation between feedforward inhibition growth and quality of hippocampal learning and memory.

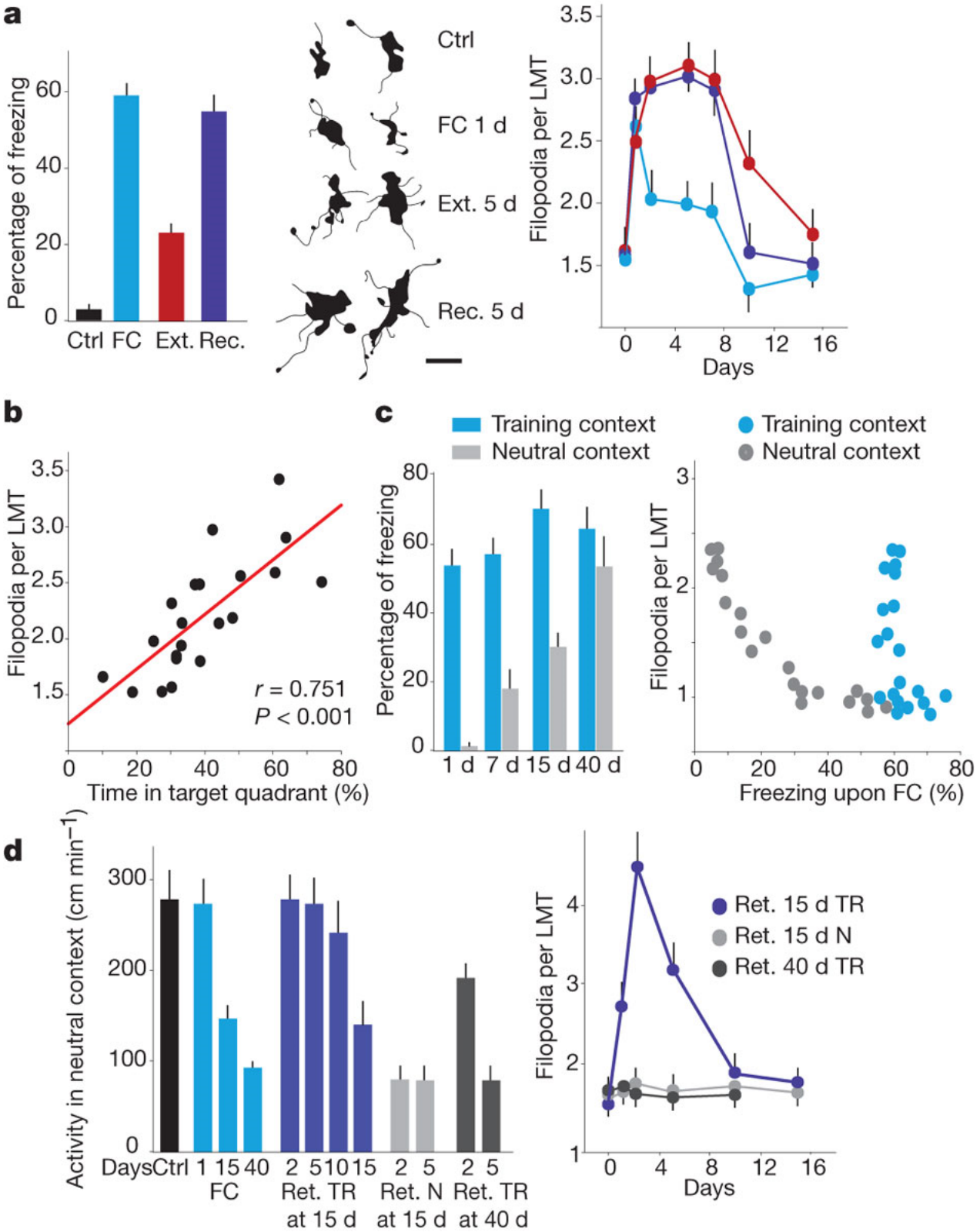

a, Memory retrieval prolongs peak levels of feedforward inhibition growth upon cued fear conditioning (FC). Pale blue: fear conditioning, no recall (at 1 day); red: fear conditioning followed by extinction (Ext.) at 5 h and 24 h (at 5 days);

violet: fear conditioning followed by recall (Rec.) at 5 h and 24 h (at 5 days). $N = 5$ mice (100 LMTs each). Scale bar, 5 μm. **b**, Correlation between reference memory precision and average filopodial contents per LMT in Morris water maze task. Dots show individual mice analysed between day 1 and day 8 of the training procedure (100 LMTs each). **c**, Time-dependent generalization upon contextual fear conditioning learning. Right, dots represent average values for individual mice at different times after fear conditioning learning (100 LMTs each). **d**, Re-growth of filopodia and re-contextualization upon retrieval of training context memory (Ret. TR) versus retrieval of neutral context (Ret. N). Left, exploratory activity in neutral context as a function of days after last manipulation. Error bars show mean ± s.e.m.

To investigate a possible functional correlate of feedforward inhibition connectivity growth, we analysed c-Fos-positive pyramidal neurons in CA3b in the contextual fear conditioning experiment[23]. On day 0, mice were exposed to the training context without or with aversive stimulus. In the absence of aversive conditioning, re-exposure on day 1 to either the training context or a neutral context produced closely comparable increases in the fractions of pyramidal neurons with high and intermediate c-Fos signals when compared to naive cage control mice (Fig. 4a). In stark contrast, association of the training context with an aversive stimulus led to a specific and robust relative increase in the number of pyramidal neurons expressing high c-Fos signals upon recall of the memory in the training context, and to a marked reduction of the high and medium c-Fos signals upon exposure to the neutral context (Fig. 4a). Recall in the training context at day 15 led to decreased high-signal c-Fos neurons, whereas exposure to a neutral context at day 15 led to markedly increased low-signal c-Fos neurons (Fig. 4b). Notably, in parallel to increased filopodial numbers and the re-establishment of memory precision, memory recall in the training context at day 15 after fear conditioning suppressed excess responses upon subsequent exposure to a neutral context (Fig. 4b).

Figure 4: Relationship between induction of c-Fos in CA3 pyramidal neurons and behavioural memory precision upon contextual fear conditioning.

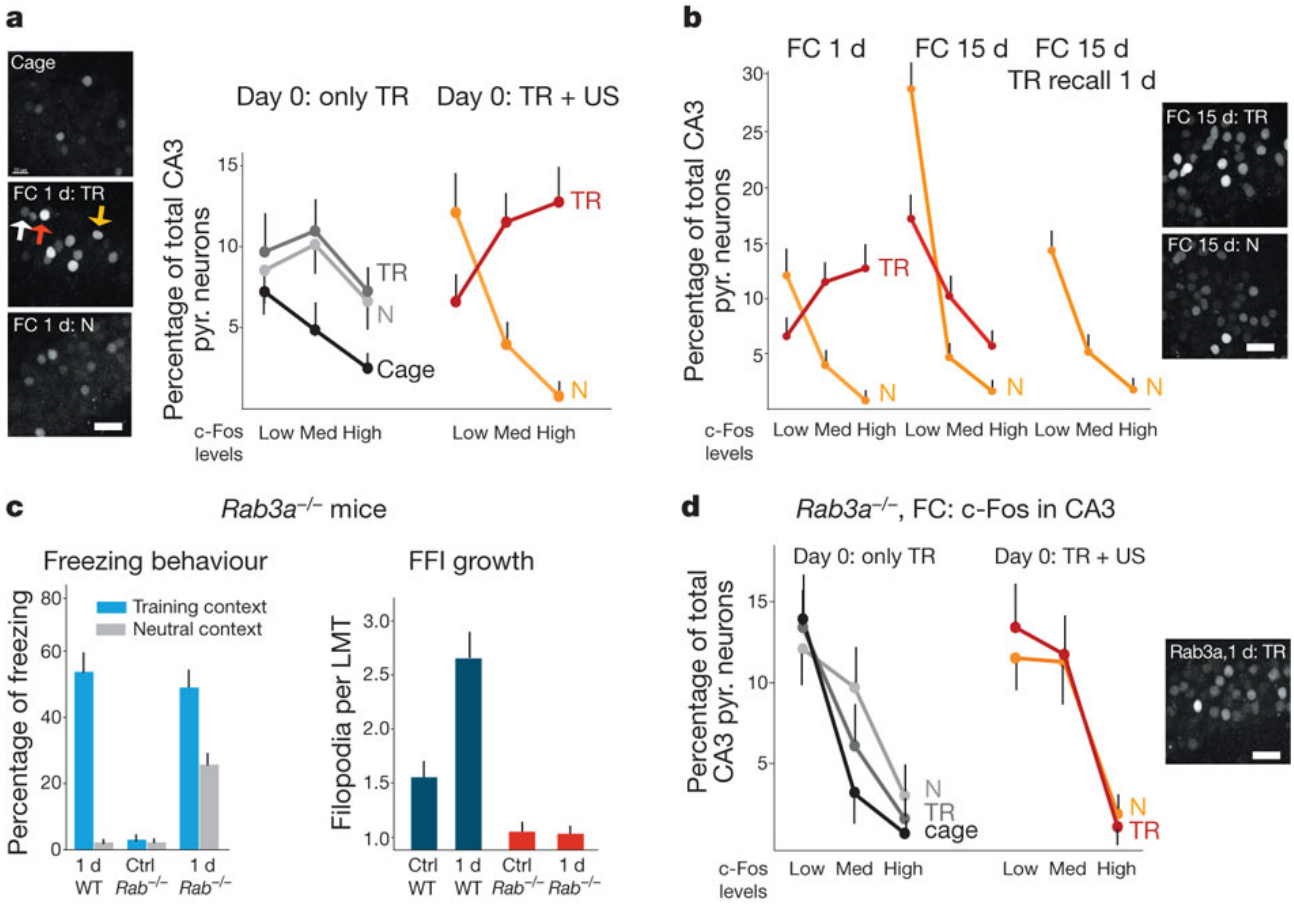

a, c-Fos immunoreactivity in CA3 pyramidal neurons upon exposure to training context (TR) or neutral context (N), with or without aversive association. Panels show representative examples of c-Fos immunoreactivity in CA3b. c-Fos neurons classified as weak (white arrow), medium (yellow arrow), strong (red arrow). $N = 3$, 500 pyramidal (pyr.) neurons each. US, unconditioned, aversive stimulus. **b**, c-Fos immunoreactivity in CA3 pyramidal neurons 15 days after fear conditioning: effect of recall with training context. Details as in **a**. $N = 1{,}000$–$1{,}500$ pyramidal neurons, from 3 mice each. **c**, Generalization and absence of learning-induced feedforward inhibition growth in *Rab3a*$^{-/-}$ mice. $N = 5$ mice (100 LMTs each). **d**, c-Fos immunoreactivity in CA3 pyramidal neurons of *Rab3a*$^{-/-}$ mice upon fear conditioning. Details as in **a**. $N = 1{,}000$–$1{,}500$ pyramidal neurons, from 3 mice each. Scale bars, 20 µm. Error bars show mean ± s.e.m.

To address the role of mossy fibres and their plasticity in fear memory precision, we carried out fear conditioning experiments in *Rab3a*$^{-/-}$ mice, which specifically lack long-term potentiation (LTP) at mossy fibres, but not at other synapses in the hippocampus[9]. We found that in the absence of Rab3a, mice learned the relationship between the training context and the aversive stimulus, but already generalized 1 day after fear conditioning (Fig. 4c). In parallel, *Rab3a*$^{-/-}$ mice lacked any learning-related increase in putative release sites at core LMTs, or any learning-related increase in filopodia numbers at LMTs in CA3 (Fig. 4c). Furthermore, analysis of c-Fos-positive neurons upon recall 1 day after learning revealed a complete absence of ensemble activity rearrangements in CA3 upon fear conditioning, leading to comparable contents of c-Fos-positive neurons upon re-exposure to the training context or exposure to an unrelated neutral context, regardless of associative learning through

aversive pairing (Fig. 4d). These results indicate that synaptic plasticity at LMTs in CA3 is required to re-organize pyramidal neuron ensemble activity in CA3 upon fear conditioning learning, to establish a precise memory of context in the hippocampus, and to induce learning-related feedforward inhibition growth.

To test the notion that learning-related feedforward inhibition growth is necessary for memory precision, we then carried out learning experiments in *Add2* knockout mice[10], which exhibit early LTP, but have a defect in synapse stabilization due to impaired linkage between the cell membrane cortex and the actin cytoskeleton[24] In naive *Add2*$^{-/-}$ mice, average values of filopodia per LMT were closely comparable to those in wild-type mice. Unlike *Rab3a*$^{-/-}$ mice, *Add2*$^{-/-}$ mice did exhibit enhanced putative release sites per core LMT upon fear conditioning (Supplementary Material), but they completely failed to establish higher numbers of filopodia upon fear conditioning (Fig. 5a). In parallel, and like *Rab3a*$^{-/-}$ mice, *Add2*$^{-/-}$ mice learned to associate fear with context, but the memory was imprecise and mice already generalized 1 day after fear conditioning (Fig. 5a). Comparable findings were obtained for Morris water maze and rotarod learning in *Add2*$^{-/-}$ mice (Fig. 5b and Supplementary Material). Absence of learning-related feedforward inhibition connectivity growth in *Add2*$^{-/-}$ mice is thus correlated with poor precision of the learned memory in the fear conditioning and Morris water maze paradigms, and with a near to complete failure to learn the rotarod task.

Figure 5: Critical role of mossy fibre Add2 for feedforward inhibition growth at LMTs and hippocampal memory precision.

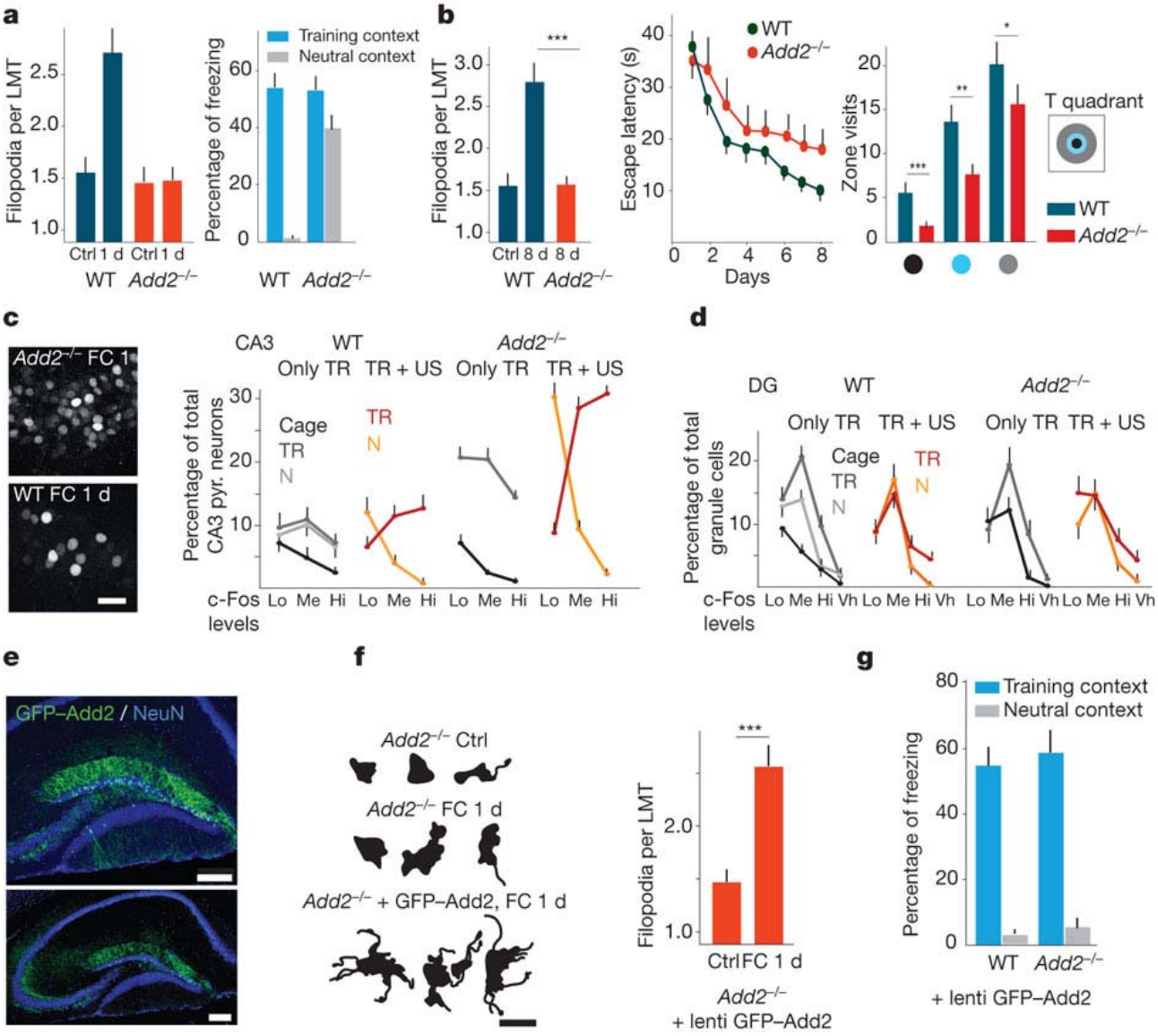

a, Absence of feedforward inhibition growth upon contextual fear conditioning, and generalization in *Add2*$^{-/-}$ mice. Conditions as in Fig. 4c. **b**, Absence of feedforward inhibition growth upon Morris water maze learning, and imprecise spatial memory in *Add2*$^{-/-}$ mice. Conditions as in Fig. 1c. **c**, **d**, c-Fos immunoreactivity in CA3 pyramidal neurons (**c**) and in dentate gyrus (DG) granule cells (**d**) of wild-type (WT) and *Add2*$^{-/-}$ mice upon exposure to training context (TR) or neutral context (N), with or without aversive conditioning. Hi, high; Lo, low; Me, medium; Vh, very high. Conditions as in Fig. 4a. **e**–**g**, Rescue of feedforward inhibition growth and contextualization upon re-expression of Add2 in granule cells of adult *Add2*$^{-/-}$ mice. **e**, Examples of transduced hippocampus (dorsal third of hippocampus). **f**, Rescue of feedforward inhibition growth; lucidas: transgene expression visualized by the GFP–Add2 construct in the absence of mGFP reporter. **g**, Behavioural rescue of contextualization. Conditions as in **a**. Scale bars: 5 μm (**f**), 20 μm (**c**) and 200 μm (**e**). Error bars show mean ± s.e.m.

We then investigated c-Fos-positive CA3 pyramidal neuron ensembles in response to fear conditioning in the *Add2*$^{-/-}$ mice. In stark contrast to *Rab3a*$^{-/-}$ mice lacking mossy fibre LTP, and consistent with increased feedforward excitation connectivity, *Add2*$^{-/-}$ mice exhibited c-Fos

ensemble reorganization responses in CA3 that were qualitatively closely comparable to those in wild-type mice (Fig. 5c). Remarkably, however, net total numbers of c-Fos-positive neurons were more than 2.5 times higher for each experimental condition in *Add2*$^{-/-}$ mice compared to wild-type mice (Fig. 5c). By contrast, numbers of c-Fos-positive pyramidal neurons in naive *Add2*$^{-/-}$ mice were not higher than those in naive wild-type mice, indicating that the mutant mice did not just exhibit raised levels of c-Fos in CA3 neurons (Fig. 5c).

In wild-type mice, a reorganization of training context/neutral context ensembles upon fear conditioning was also detected in granule cells, but it was much less marked than in CA3 (Fig. 5d). Notably, however, and in stark contrast to CA3, distributions and numbers of c-Fos positive granule cells in *Add2*$^{-/-}$ mice were not different from those in wild-type mice for all experimental conditions tested (Fig. 5d). Therefore, *Add2*$^{-/-}$ mice re-organized their CA3 pyramidal neuron ensembles like wild-type mice, but failed to restrict the numbers of activated pyramidal neurons in CA3 upon stimuli, which is consistent with a complete absence of feedforward inhibition connectivity growth at LMTs. Furthermore, c-Fos activation patterns in CA3 correlated with memory precision, whereas those in dentate gyrus did not, suggesting that the absence of Add2 in mossy fibres and their LMTs may account for the impaired memory precision in *Add2*$^{-/-}$ mice.

To establish a causal link between learning-related feedforward inhibition growth at LMTs and memory precision, we determined whether re-expression of Add2 specifically in granule cells and their mossy fibres was sufficient to rescue filopodial growth and memory precision upon fear conditioning. To achieve specific re-expression in the adult, we expressed Add2 selectively in the dentate gyrus[15] of *Add2*$^{-/-}$ mice using a lentiviral construct. One month after viral transduction, 15–22% of granule cells throughout the entire hippocampus exhibited virus-driven gene expression, whereas expression outside the dentate gyrus was extremely rare (Fig. 5e). The re-introduction of Add2 in mossy fibres was sufficient to rescue filopodial growth at LMTs of transduced granule cells in response to fear conditioning (Fig. 5f). Most notably, and in parallel to restored feedforward inhibition growth, re-expression of Add2 in granule cells rescued behavioural contextualization upon fear conditioning (Fig. 5g).

Our results establish a causal relationship between learning-associated structural alterations in identified circuit connectivity and a specific behavioural output. We provide evidence that increased feedforward inhibition connectivity upon learning by mossy fibre LMTs in CA3 is critically important for the behavioural precision of learning-related hippocampal spatial memories. We further show that, upon learning, the increased feedforward inhibition connectivity is brought about through structural plasticity at a substantial fraction of LMTs in CA3, leading to about a doubling in the numbers of excitatory synapses onto parvalbumin-positive inhibitory interneurons (see also Supplementary Material).

Our results introduce a distinction between spatial learning, which is present in *Add2*$^{-/-}$ mice, and the behavioural precision of the learning, which is compromised in these mutant mice. The distinction is consistent with the notion that the hippocampus is critically important for the precision of contextual memorie[25]. Within the hippocampal circuit, the dentate gyrus establishes fine-grained representations of experience, which it transmits to CA3 (ref. 13). Upon learning-induced potentiation, this high-resolution information may augment the detection of similarities among unrelated events through the associational network in CA3. Accordingly, filtering of the mossy fibre output through feedforward inhibition connectivity upon learning[26,27,28] may support memory precision by restricting the extraction of relational representations in CA3 (ref. 29). The increase in feedforward inhibition

connectivity through structural plasticity discovered in this study may thus have important roles in ensuring the precision of behaviourally relevant memories upon learning, under normal and pathological conditions.

METHODS SUMMARY

Rab3a$^{-/-}$ and *Add2*$^{-/-}$ mice[9,10] were fromJackson Laboratories; the reporter line *Thy1-mGFP(Lsi1)* was as described before[5]. The membrane-targeted green fluorescent protein (mGFP) lentivirus to trace mossy fibre projections was as described previously[15]; the GFP–Add2 construct was cloned into a lentivirus vector, and dentate gyrus infections were as described previously[15].

For anatomical analysis, mice were perfused with ice-chilled 4% paraformaldehyde in 0.1MPBS, and brains were post-fixed. Hippocampi were mounted in 3% agarose blocks, and 100-mm transversal sections of hippocampi were cut using a McIlwain tissue chopper. Sections analysed were within 15% and 30% along the anterior–posterior axis. All LMTs that could be resolved in three dimensions within any given optical field (3100) were analysed for filopodial contents. Filopodia were defined as processes emanating from LMTs of at least 2 μm length; varicosities were defined as end-swellings of at least 1 μm in diameter.

The immuno-electron microscopy analysis was performed according to a published procedure[30].

For c-Fos analysis, mice were perfused for 90 min after the last memory recall. Quantitative analysis of Bassoon puncta and c-Fos-positive nuclei was performed using a computerized image analysis system (Imaris 7, Bitplane). Nucleiwere detected automatically as spheres of 8 μm, and the software yielded distributions of c-Fospositive nuclei. Intensity thresholds for CA3 were defined as follows: low (>280, <450), medium (>450, <700), high (>700; the highest values were about 1,400).

Statistical analyses were performed using Student's *t*-tests and one-way ANOVA; post hoc comparisons were at the $P < 0.05$ level of significance. Results are presented as mean ± s.e.m.

All behavioural experiments were carried out with male mice that were 55–65 days old at the onset of the experiment, and were according to standard procedures. All subsequent morphological and immunohistochemical analyses of behaviourally treated mice were carried out blind to behavioural conditions.

METHODS

Reagents and immunocytochemistry

Antibodies were from the following sources, and were used as follows: parvalbumin, Swant, 1:5,000; VGluT1, SySy, 1:1,000; GAD65/67, Millipore, 1:1,000; c-Fos, Santa Cruz, 1:10,000; NeuN, Chemicon, 1:200; Bassoon, Millipore, 1:200; Alexa-labelled secondary antibodies, Molecular Probes, 1:500.

For immunocytochemistry, tissues were permeabilized with 0.2% Triton X-100 in PBS with 10% bovine serum albumin (BSA). Antibody incubations were overnight at 4 °C.

Fluorescence was imaged on either an upright spinning disk microscope consisting of a Yokogawa CSU22 confocal scanning head mounted on a Zeiss Axioimager M1 using a ×100 alphaPlan-

Apochromat 1.45 (Zeiss) oil-immersion objective, or on an LSM510 confocal microscope (Zeiss) using a ×63 (1.4) oil-immersion objective.

At least four sections were analysed per mouse, and the data are based on 300–500 μm regions along the anterior–posterior axis.

c-Fos analysis

For c-Fos analysis, all samples belonging to the same experimental set were processed in parallel. Occasional sections in which NeuN signals were lower than average, or where c-Fos signal intensities varied within different regions of the section were discarded as technically poor. All images were acquired with the same settings, which were defined in order to avoid saturation of the highest c-Fos signals in CA3 and dentate gyrus, and to still detect background levels outside cell clusters. Cells were binned according to labelling intensities using an automatic procedure, and the same threshold settings were used for all experiments. For dentate gyrus granule cells, the thresholds were as follows: low (>280, <450), medium (>450, <700), high (>700, <1,000), very high (>1,000; the highest values were about 2,200). c-Fos immunoreactive neurons were counted using a minimum of four sections per animal, and normalized to the total number of NeuN-positive nuclei within the neuronal layers in CA3 or dentate gyrus. In a first series of experiments, batches of naive and fear conditioning control mice (training context without unconditioned aversive stimulus) were tested for inter-animal variability, which was found to be very low.

Behavioural experiments

The behavioural experiments were in accordance with institutional guidelines, and were approved by the Veterinary Department of the Canton of Basel-Stadt. Mice were kept in temperature-controlled rooms on a constant 12 h light/dark cycle, and experiments were conducted at the approximate same time during the light cycle. Before the behavioural experiments, mice were kept in a holding room in single cages for 3–4 days. At the onset of each behavioural experiment mice were 50–60 days old.

For the Morris water maze test, the 140 cm pool was surrounded by black curtains, and by four different objects. A circular escape platform (10 cm diameter) was submerged 0.5 cm below the water surface, and was kept in a fixed position. Mice were trained to find the platform for 4 trials a day, during up to 8 days. During training, mice were released from pseudo-randomly assigned start locations; they were allowed to swim for up to 60 s, when they were manually guided to the platform in the case of failures. Inter-trial intervals were 5 min. Single probe trials to test reference memory were conducted 1 day after the last training session. Mice were released at a random start position, and were allowed to swim during 60 s in the absence of the platform.

The training context (TR) was rectangular, and was cleaned with 1% acetic acid before and after each trial; the neutral context (N) had a cylindrical shape and was cleaned with 70% ethanol. Freezing was defined as the absence of somatic motility, except for respiratory movements. Exploratory activity was measured as body distance travelled over time. Once placed in the conditioning chamber, the mice were allowed to freely explore for 2.5 min, and they received 5 presentation of conditioned stimulus and unconditioned stimulus (1 s foot shock, 0.8 mA; where indicated, 10 kHz tone for 10 s, 70 dB sound pressure level, inter-trial interval 30 s). The last 1 s of each tone was paired with the unconditioned stimulus. Contextual fear conditioning involved the same protocol, but without the tone component. To test for contextual fear memory, mice were returned to training (or neutral) context during a test period of 2.5 min. To test for cued fear conditioning, mice explored for 2 min, followed by 5 tone presentations. The test was performed either in the conditioning context (context- and tone-dependent freezing), or in a novel context (tone-dependent freezing).

To test for context discrimination after fear conditioning, a within-subjects design was used. On the test day, freezing was assessed in training context during 2.5 min, and 5 h later in neutral context. Where indicated, mice were tested for generalization in neutral context, followed 5 h and 24 h later by two brief recall sessions (in training or neutral context). Subsequently, discrimination was tested in a second novel context (novel room shape; 0.25% benzaldehyde/ethanol).

Data from training sessions and probe trials were collected and analysed using Viewer2 Software (Biobserve). Cued and contextual fear conditioning were carried out in the Mouse Test Cage (Coulbourn Instruments). Freezing behaviour was scored using Ethovision software (Noldus). Mice were excluded from the data set if they failed at the behavioural analysis; this was the case when mice failed to extinguish fear responses to training context (two mice), exhibited weak freezing to training context in the recall experiments at day 15 (three mice), exhibited signs of behavioural extinction upon recall of training context at day 15 (seven mice), or failed to learn the Morris water maze (one mouse).

Transmission electron microscopy

This procedure is described in detail elsewhere[30]. Briefly, mice were transcardially perfused with 2% paraformaldehyde and 0.2% glutaraldehyde in PBS 0.1 M pH 7.4. Right and left hippocampi were dissected, and 60 µm vibratome (Leica) sections were obtained, rinsed, cryoprotected and freeze-thawed in liquid nitrogen. Sections were incubated in first antibody (GFP, chemicon 1:1,000) overnight, followed by biotinylated secondary antibody (Invitrogen 1:500). After incubation in the avidin-biotin peroxidase complex (ABC elite, Vector Laboratories), labelling was performed with DAB and hydrogen peroxide. After the revelation of the labelling, sections were stained in osmium tetroxide and dehydrated. After impregnation with Durcupan resin (FLUKA) sections were flat-embedded between two silicon-coated glass slides and cured in a 60 °C oven for 48 h.

Transmission light microscopy was performed in stratum lucidum to search for large mossy fibre terminals with more than three filopodia. Appropriate blocks were then trimmed, and 60 nm serial sections were cut and collected on formvar coated slot-grids. Images of labelled terminal were acquired with a side-mounted digital camera (Veleta, Olympus) on a Philips CM10 transmission electron microscopy at 80 kV, and a pixel size of 2.63 nm. To reconstruct the structure in three dimensions, images were aligned (Autoaligner, Bitplane), and contours were drawn manually using Imaris 7.1.2 (Bitplane). Surface rendering was achieved using Geometry converter (J. Wolf) and Blender.

Acknowledgements

We thank S. Arber and B. Roska for valuable comments on the manuscript.Weare grateful to J. Pielage for sharing with us his findings on the function of Add2 in synapse stability, and to G. Courtine for advice on the c-Fos labelling protocol. The Friedrich Miescher Institut is part of the Novartis Research Foundation.

Contributions

S.R. devised, carried out and analysed all experiments except for those of Fig. 2a–c, part of Fig. 2d, Fig. 5a, e–g and Supplementary Fig. 4; C.V. carried out the experiments of Fig. 2a–c, part of Fig. 2d and Supplementary Fig. 4; E.B. devised and carried out the behavioural and rescue experiments on Add22/2 mice; C.G. carried out the immuno-electron microscopy experiments; B.S. provided advice in planning and interpreting the fear conditioning experiments; P.S. provided advice on the cerebellar experiments; P.C. helped devise the experiments and wrote themanuscript. All authors discussed the results and commented on the manuscript.

Competing financial interests

The authors declare no competing financial interests.

Corresponding author

Correspondence and requests for materials should be addressed to Pico Caroni (caroni@fmi.ch).

REFERENCES

1. Holtmaat, A. & Svoboda, K. Experience-dependent structural plasticity in the mammalian brain. Nature Rev. Neurosci. 10, 647–658 (2009).
2. Hu¨bener, M.&Bonhoeffer, T. Searching for engrams. Neuron67, 363–371 (2010).
3. Lamprecht, R.& LeDoux, J. Structural plasticity andmemory. Nature Rev. Neurosci. 5, 45–54 (2004).
4. Wilbrecht, L., Holtmaat, A., Wright, N., Fox, K. & Svoboda, K. Structural plasticity underlies experience-dependent functional plasticity of cortical circuits. J. Neurosci. 30, 4927–4932 (2010).
5. DePaola, V., Arber, S.&Caroni, P.AMPAreceptors regulate dynamicequilibriumof presynaptic terminals in mature hippocampal networks. Nature Neurosci. 6, 491–500 (2003).
6. Hofer, S. B., Mrsic-Flogel, T. D., Bonhoeffer, T. & Hu¨bener, M. Experience leaves a lasting structural trace in cortical circuits. Nature 457, 313–317 (2009).
7. Xu, T. et al. Rapid formation and selective stabilization of enduring motor memories. Nature 462, 915–919 (2009).
8. Yang, G., Pan, F. & Gan, W. B. Stably maintained dendritic spines are associated with lifelong memories. Nature 462, 920–924 (2009).
9. Castillo, P. E. et al. Rab3A is essential for mossy fibre long-term potentiation in the hippocampus. Nature 388, 590–593 (1997).
10. Rabenstein, R. L. et al. Impaired synaptic plasticity and learning in mice lacking b-adducin, an actin-regulating protein. J. Neurosci. 25, 2138–2145 (2005).
11. Wang, S.-H. & Morris, R. G. Hippocampal-neocortical interactions inmemory formation, consolidation,andreconsolidation.Annu.Rev.Psychol. 61,49–79 (2010).

12. Nakashiba, T., Young, J. Z., McHugh, T. J., Buhl, D. L. & Tonegawa, S. Transgenic inhibition of synaptic transmission reveals role of CA3 output in hippocampal learning. Science 319, 1260–1264 (2008).
13. Leutgeb, J. K., Leutgeb, S., Moser, M. B. & Moser, E. I. Pattern separation in the dentate gyrus and CA3 of the hippocampus. Science 315, 961–966 (2007).
14. Gogolla, N., Galimberti, I., Deguchi, Y. & Caroni, P. Wnt signaling mediates experience-related regulation of synapse numbers and mossy fiber connectivities in the hippocampus. Neuron 62, 510–525 (2009).
15. Galimberti, I., Bednarek, E., Donato, F. & Caroni, P. EphA4 signaling in juveniles establishes topographic specificity of structural plasticity in the hippocampus. Neuron 65, 627–642 (2010).
16. Acsady, L., Kamondi, A., Sik, A., Freund, T. & Buszaki, G. GABAergic cells are the major postsynaptic target of mossy fibers in the rat hippocampus. J. Neurosci. 18, 3386–3403 (1998).
17. Lawrence, J. J. & McBain, C. J. Interneuron diversity series: containing the detonation—feedforward inhibition in theCA3 hippocampus. Trends Neurosci. 26, 631–640 (2003).
18. Mori, M., Abegg, M. H., Gaehwiler, B. H. & Gerber, U. A frequency-dependent switch from inhibition to excitation in a hippocampal unitary circuit. Nature 431, 453–456 (2004).
19. D'Angelo, E. & De Zeeuw, C. I. Timing and plasticity in the cerebellum: focus on the granular layer. Trends Neurosci. 32, 30–40 (2009).
20. Sacchetti, B., Scelfo, B., Tempia, F. & Strata, P. Long-term synaptic changes induced in the cerebellar cortex by fear conditioning. Neuron 42, 973–982 (2004).
21. Wiltgen, B. J. & Silva, A. J. Memory for context becomes less specific with time. Learn. Mem. 14, 313–317 (2007).
22. Biedenkapp, J. C. & Rudy, J. W. Context pre-exposure prevents forgetting of a contextual fear memory: implication for regional changes in brain activation patterns associated with remote and recent memory tests. Learn. Mem. 14, 200–203 (2007).
23. Kubik, S., Miyashita, T. & Guzowski, J. F. Using immediate-early genes to map hippocampal subregional functions. Learn. Mem. 14, 758–770 (2007).
24. Bednarek,E.&Caroni, P.b-Adducin is requiredfor stableassembly ofnewsynapses and improved memory upon environmental enrichment. Neuron. (in the press).
25. Wiltgen, B. J. et al. The hippocampus plays a selective role in the retrieval of detailed contextual memories. Curr. Biol. 20, 1336–1344 (2010).
26. Lamsa, K., Heeroma, J. H. & Kullmann, D. M. Hebbian LTP in feed-forward inhibitory interneurons and the temporal fidelity of input discrimination. Nature Neurosci. 8, 916–924 (2005).
27. Wulff, P. et al. Synaptic inhibition of Purkinje cells mediates consolidation of vestibulo-cerebellar motor learning. Nature Neurosci. 12, 1042–1049 (2009).
28. Pouille, F., Marin-Burgin, A., Adesnik, H., Atallah, B. V. & Scanziani, M. Input normalization by global feedforward inhibition expands cortical dynamic range. Nature Neurosci. 12, 1577–1585 (2009).
29. McNaughton, B. L. & Morris, R. G. M. Hippocampal synaptic enhancement and information storage within a distributed memory system. Trends Neurosci. 10, 408–415 (1987).
30. Knott, G. W.,Holtmaat, A., Trachtenberg, J. T., Svoboda, K.&Welker, E.Aprotocol for preparingGFP-labeled neurons previously imaged in vivoandin slice preparations for lightandelectronmicroscopicanalysis. Nature Protocols 4,1145–1156 (2009).

doi:10.1038/nature09946

Introduction hippocampus:

The hippocampus accounts for the rapid generation and contextualization of episodic memories[21,22]. Within the main hippocampal circuit, the subregion CA3 establishes links between the modalities of individual episodes, and between related episodes through its auto-associational network[21,23]. The mossy fiber projection, which consists of the axons of glutamatergic dentate gyrus granule cells, conveys highly contextualized information from the dentate gyrus onto CA3 through its Large Mossy fiber Terminals (LMTs; Fig. 1a)[24]. These mediate powerful monosynaptic feedforward excitation onto pyramidal neurons through their core terminals, and di-synaptic feedforward inhibition through filopodia that emanate from the terminals. The filopodial synapses excite inhibitory interneurons, which in turn inhibit the pyramidal neurons in CA3 (Fig. 1a)[12]. For simplicity, we designated the filopodia synapses as feedforward inhibition connectivity. The plasticity and connectivity properties of this feedforward excitation/feedforward inhibition arrangement are thought to ensure shunting of pyramidal neuron excitation at low activation levels of the mossy fibers, and recruitment of small ensembles of pyramidal neurons under conditions of high activation (Suppl. Fig. 1)[13,25,26].

FFI growth in hippocampus and cerebellum:

Analysis of axons: The main findings of this study were confirmed in mice in which hippocampal mossy fibers were labeled upon transduction with an mGFP-lentivirus (not shown)[11].

Filopodial growth: Upon fear conditioning, filopodial growth was rapid: it reached peak values at 1h, and these values were maintained during 1-1.5 days after fear conditioning (Fig. 1c). Subsequently, filopodial contents decreased to intermediate values (about 1.3-fold higher than baseline levels), and decreased again to reach naive values at 8-10 days (Fig. 1c, Suppl. Fig. 2a). In control mice and 1d after fear conditioning, about 50% of the filopodia exhibited varicosities larger than 1 μm in diameter, which in more than 95% of the cases were associated with Bassoon-positive active zone puncta (Fig. 1d, Suppl. Fig. 3b).

Filopodial synapses: At 1h, and to a lesser extent at 6h after fear conditioning, slightly larger fractions of filopodia lacked varicosities with Bassoon-positive puncta, suggesting that the formation of new synapses went on during several hours after fear conditioning (Fig. 1d, Suppl. Fig. 3b). The more modest increase in feedforward excitation connectivity at LMTs also developed within 1h upon fear conditioning, but was more long lasting than the increase in feedforward inhibition connectivity (Suppl. Fig. 2a). When the protein synthesis inhibitor anisomycin was administered shortly before learning, it suppressed both consolidation of the fear memory and the increase in filopodia numbers (Suppl. Fig. 2b), suggesting that the filopodial growth occurred as part of the memory consolidation process[22].

Morris water maze learning: During the 8 days Morris water maze protocol, mice learn to locate a fixed hidden platform position, starting from any point at the edge of the pool. Like fear conditioning, the protocol involves hippocampus-dependent spatial learning, but unlike fear conditioning the learning process is incremental[12]. Latencies to find the hidden platform exhibited a bi-modal curve: mice improved rapidly, but exhibited a pronounced variability within the first 3-4 days, whereas further improvement during the next 3-4 days led to low variability plateau levels of performance at 7-8 days (Fig. 1g). In parallel, the mice established enhanced numbers of filopodia at LMTs (Fig. 1g).

Rotarod learning: Upon termination of the training at day 7, the motor skill was gradually lost over a period of 15-20 days, and so were the excess filopodia (Fig. 2b). Since the possible targets of mossy fiber terminal filopodia in cerebellar cortex had not been identified, we investigated the possibility that these filopodia may make synaptic contacts with Golgi cells, i.e. the fast-spiking interneurons that convey feedforward inhibition to cerebellar granule cells[14,27].

Filopodial growth specifically associated with learning: To further investigate the specificity relating learning to feedforward inhibition connectivity growth, we analyzed hippocampal CA3 and the cerebellar lobules 5 and 9 in mice that had been subjected to different behavioral experiences. Consistent with the existence of contextual components in the cued fear conditioning experiment, this protocol led to filopodial growth both in dorsal hippocampus and in cerebellar lobule 5 (Fig. 2d). By contrast, contextual fear conditioning or Morris water maze learning did not produce filopodial growth in cerebellar lobules 5 or 9 (Fig. 2d). In addition,

rotarod training affected filopodial numbers in cerebellar lobule 9, but not in dorsal hippocampus (Fig. 2d). Finally, housing mice under environmentally enriched conditions, which leads to enhanced motor activity and improved potential for learning, but does not by itself involve any specific skill learning, did not affect filopodial numbers in dorsal hippocampus nor in the cerebellum (Fig. 2d). Therefore, feedforward inhibition connectivity growth is specifically correlated to learning, and is confined to brain structures involved in that learning paradigm.

Function of FFI growth:

Feedforward inhibition can restrict and temporally sharpen the spread of excitatory activity in CA3[11] and in the granule cell layer of cerebellar cortex[14,27], suggesting that the feedforward inhibition growth might support precision in the behavioral expression of the memory[14,26].

Extinction and recall: To further investigate how filopodial growth relates to behavioral expression of the fear memory, we elicited extinction of cued and contextual fear conditioning by repeatedly re-exposing mice to training context (TR) and tone (20 times) without the aversive stimulus, 5h and 24h after fear conditioning. This protocol produced behavioral extinction of the fear response, but instead of reducing filopodial numbers at hippocampal LMTs, it prolonged peak filopodial responses from 1 to 4-6 days (Fig. 3a). Re-exposing mice briefly to TR, and to one tone instead of twenty at 5h and at 24h did not extinguish the fear response, but also extended peak filopodial response values to 4-6 days (Fig. 3a), suggesting that the temporal extension of excess filopodia was induced by recall of the fear-associated memory.

Filopodial growth upon fear conditioning protocols : With our fear conditioning protocol, recall at 40 days only partially reduced generalization during 2-3 days[22], and did not induce feedforward inhibition growth (Fig. 3d). Time-dependent generalization is typically most pronounced upon fear conditioning protocols like the one used in this study, which did not involve previous familiarization of the mice with TR[16,17]. Indeed, when mice were pre-exposed to TR for 5 min on the day before learning, the decline in learning-induced filopodial growth was delayed, and so was the loss of memory precision (Suppl. Fig. 5). Taken together, the results of these behavioral experiments provide correlative evidence that learning-related feedforward

inhibition growth at the mossy fiber projection in CA3 might support the precision of hippocampus-dependent memories[19].

Functional correlate of FFI growth (c-Fos):

c-Fos ensemble reorganization in CA3: Consistent with robust behavioral precision, association of the training context TR with the aversive stimulus led to an organization of the cell ensemble in CA3 upon memory recall that was very different from the ensemble in the conditioning control group (TR alone): fear memory formation to TR resulted in strong c-Fos responses specifically to fear-related context (TR), and in suppressed responses to a novel context (N). Taken together, these results are consistent with the hypothesis that decreased LMT filopodial contents paired to persistent hippocampal memory lead to high numbers of c-Fos positive neurons recruited by a novel context N in CA3 and a loss of fear memory precision. The results further suggest that retrieval-induced feedforward inhibition growth restricts the ensemble of CA3 pyramidal neurons recruited by unrelated context, thus supporting precision of the learned fear.

c-Fos 15d upon fear learning: As shown in Fig. 3c, exposure to TR elicited comparable freezing responses at 1d and 15d after fear conditioning, but at 15d filopodia levels had returned to control values and discrimination against a novel context N had decreased. In parallel, recall in TR at 15d led to decreased high-signal c-Fos neurons, whereas exposure to N at 15d led to dramatically increased low-signal c-Fos neurons (Fig. 4b). Notably, in parallel to increased filopodial numbers and the re-establishment of memory precision, memory recall in TR at 15d after fear conditioning suppressed excess responses upon subsequent exposure to a novel context N (Fig. 4b).

Synapse growth at LMTs in the absence of Rab3a: *Rab3a*$^{-/-}$ mice lacked any learning-related increase in putative release sites at core LMTs (feedforward excitation connectivity; *Rab3a*$^{-/-}$: 5.61$\pm$0.08 (control) versus 5.62$\pm$0.07 (fear conditioning, 1d) Bassoon positive puncta per 10 μm^3 of LMT volume; wildtype: 5.48$\pm$0.08 (control) versus 7.18$\pm$0.11(fear conditioning, 1d); N=60 LMTs from 3 mice each), or any learning-related increase in filopodia numbers at LMTs in CA3 (feedforward inhibition connectivity; Fig. 4c).

LMT densities in *Rab3a*$^{-/-}$ mice were identical to those in wildtype mice (average LMT distances in CA3b were 98.2±2.1 μm (wildtype) and 100.4±2.3 μm (*Rab3a*$^{-/-}$); N=60 terminal pairs, from 3 mice each).

Synapse growth at LMTs in the absence of β-Adducin: Unlike *Rab3a*$^{-/-}$ mice, *β–Adducin*$^{-/-}$ mice did exhibit enhanced putative release sites per core LMT upon fear conditioning (feedforward excitation connectivity; 5.64±0.11 (control) versus 6.62±0.15 (fear conditioning 1d) Bassoon positive puncta per 10 μm^3 of LMT volume; N=60 LMTs from 3 mice each). However, *β–Adducin*$^{-/-}$ mice completely failed to establish higher numbers of filopodia upon fear conditioning (feedforward inhibition connectivity; Fig. 5a). LMT densities in *β-Adducin*$^{-/-}$ mice were identical to those in wildtype mice (average LMT distances in CA3b were 98.2±2.1 μm (wildtype) and 98.1±1.8 μm (*β-Adducin*$^{-/-}$); N=60 terminal pairs, from 3 mice each). LMT densities in *β-Adducin*$^{-/-}$ mice were identical to those in wildtype mice (average LMT distances in CA3b were 98.2±2.1 μm (wildtype) and 98.1±1.8 μm (*β-Adducin*$^{-/-}$); N=60 terminal pairs, from 3 mice each).

Morris water maze and rotarod learning in the absence of β-Adducin: In a second set of experiments we carried out Morris water maze spatial learning experiments in *β–Adducin*$^{-/-}$ mice. Again, *β–Adducin*$^{-/-}$ mice exhibited no learning-related increase in the content of filopodia per LMT (Fig. 5b). Mutant mice learned to locate the platform and established a reference memory of the correct quadrant (Fig. 5b). However, the characteristic improvements beyond 3-4 days were absent, and when the precision of the reference spatial memory was assessed by a quantitative analysis of swimming behavior as a function of platform position, mice lacking β-Adducin were clearly impaired (Fig. 5b). In a third set of experiments we determined whether *β–Adducin*$^{-/-}$ mice may also be impaired in learning-related filopodial growth at cerebellar mossy fiber terminals, and if so how that might affect cerebellar learning. We found that *β–Adducin*$^{-/-}$ mice failed to establish extra filopodia at lobule 9 mossy fiber terminals upon rotarod training (Suppl. Fig. 6). In parallel, mice lacking β-Adducin were greatly impaired in learning the rotarod task (Supp. Fig. 6).

c-Fos in granule cells: If the absence of feedforward inhibition connectivity growth at LMTs accounts for the excess of c-Fos positive CA3 pyramidal neurons upon fear conditioning in *β–Adducin*$^{-/-}$ mice, then the activation excess may be absent in the neurons of origin of the LMTs, i.e. dentate gyrus granule cells. Accordingly, to determine whether it was c-Fos positive neuronal ensembles in CA3 that were specifically enlarged in *β–Adducin*$^{-/-}$ mice, we also analyzed c-Fos positive dentate gyrus granule cells in the fear conditioning experiments.

Relating feedforward inhibition growth and c-Fos ensembles: Consistent with the notion that the absence of feedforward inhibition connectivity growth at LMTs of *β–Adducin*$^{-/-}$ mice may account for the excess of c-Fos positive neurons under our experimental conditions, filopodia/LMT distributions in the mutant mice after learning were comparable to naïve, and not to TR control (no aversive stimulus) wild-type mice (Suppl. Fig. 7). In experiments aimed at further investigating how feedforward excitation and feedforward inhibition connectivity ratios at LMTs influence CA3 pyramidal neuron recruitment, we analyzed mice that had been housed under environmental enrichment conditions, a procedure leading to markedly enhanced contents of Bassoon puncta at core LMTs[27], but not to higher filopodial contents at LMTs (Fig. 2d). Consistent with the notion that enhanced levels of Bassoon puncta at core LMTs in the absence of a corresponding increase in filopodial synapses can produce elevate levels of c-Fos positive neurons in CA3, enriched mice exhibited c-Fos positive ensembles in CA3 that were markedly higher than those of mice housed under control conditions (Suppl. Fig. 8).

Discussion:

Our findings suggest that the absence of mossy fiber LTP in *Rab3a*$^{-/-}$ mice may compromise memory precision by failing to induce learning-induced re-organization of CA3 ensemble activity. This interpretation is consistent with the strikingly low contents of high- and medium-signal c-Fos positive neurons in the *Rab3a*$^{-/-}$ mice, and suggests that mossy fiber LTP has an important role for the behavioral precision of learning-related hippocampal memories. By contrast, in *β–Adducin*$^{-/-}$ mice ensemble re-organization was normal in CA3, but the sizes of c-Fos positive neuronal ensembles were greatly enlarged, and memory precision was again impaired. The absence of increased feedforward inhibition connectivity in *β–Adducin*$^{-/-}$ mice may thus compromise memory precision by failing to globally restrict network activity upon learning,

thereby allowing otherwise sub-threshold partial stimuli to produce memory retrieval[26,28] (Suppl. Fig. 1). Consistent with this interpretation, elevated core LMT levels of Bassoon positive puncta persisted upon fear conditioning in wildtype mice after the extra filopodia had vanished (Suppl. Fig. 2a), time-dependent loss of the excess filopodial synapses coincided with behavioral generalization of the fear memory (Fig. 3c), and retrieval of the specific training context memory restored the excess filopodia and memory precision (Fig. 3c). This latter finding further suggests that upon filopodial retraction the specific memory did persist, within and/or outside the hippocampus, but activity patterns in CA3 elicited by a novel context were not sufficiently filtered to prevent behavioral generalization. A plausible interpretation of our findings is that retrieval and reconsolidation of the training memory through the hippocampal circuit re-activates plasticity sufficient to re-induce feedforward inhibition growth and a high-threshold for subsequent activity flow[26,29]. The extent to which this process is intrinsic to the hippocampus remains to be determined.

Feedforward inhibition growth and memory recall: The interpretation of our findings as described in the last paragraph of the manuscript is in line with the results of recent physiological studies, which have provided evidence that feedforward inhibition mainly acts to globally reduce network activity, without affecting relative activity patterns[30]. The interpretation is further reminiscent of early theoretical proposals suggesting that low activation thresholds upon LTP may prevent "perfect recall" within hippocampal networks through saturation processes, and that the recruitment of feedforward inhibition circuitry may be well suited to keep activation thresholds within sub-saturation ranges[30].

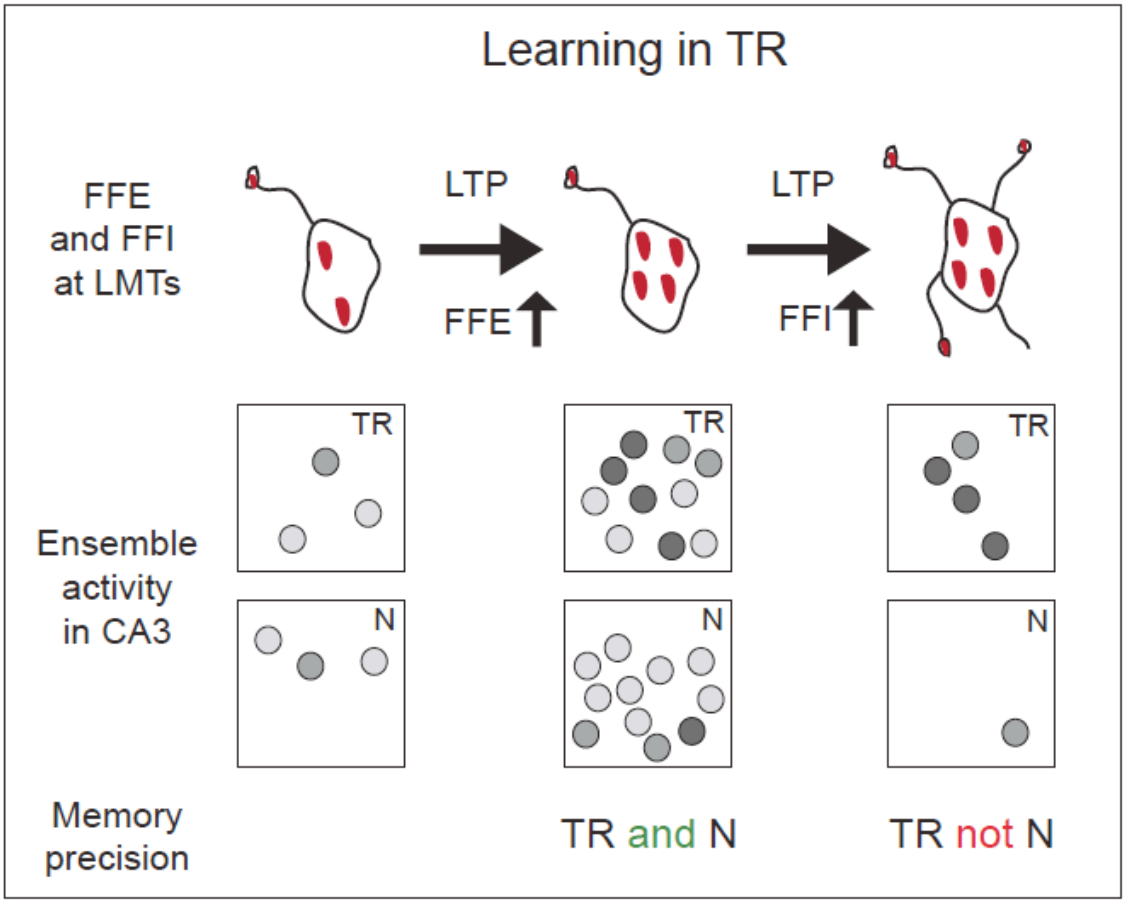

Supplementary Figure 1

Learning-related feedforward inhibition connectivity growth required for memory precision. The schematic summarizes the main finding of this study. Upper row: Learning-related feedforward excitation (FFE) and feedforward inhibition (FFI) growth at hippocampal mossy fiber terminals. Upon hippocampus-dependent learning, Rab3a-dependent mossy fiber LTP leads to enhanced numbers of active zones at core LMTs (enhanced FFE, center), and to β-Adducin-dependent higher numbers of filopodia (enhanced FFI connectivity, right). Red spots: synaptic sites at core LMTs and filopodial varicosities. Middle row: In the absence of learning, the different contexts TR and N elicit comparable numbers of c-Fos positive pyramidal neurons in CA3 (left). Learning produces mossy fiber LTP- and β-Adducin-dependent re-organization of activated ensembles in CA3, leading to substantially augmented recruitment of pyramidal neurons upon re-exposure to training context TR, and suppressed recruitment upon exposure to novel context N (right). In the absence of FFI growth, LTP and ensemble re-organization produce an excess of recruited pyramidal neurons in CA3 (center). Darker grey tones indicate higher levels of c-Fos accumulation in individual pyramidal neurons. Lower row: FFI growth is required for behavioral discrimination between TR and N upon learning.

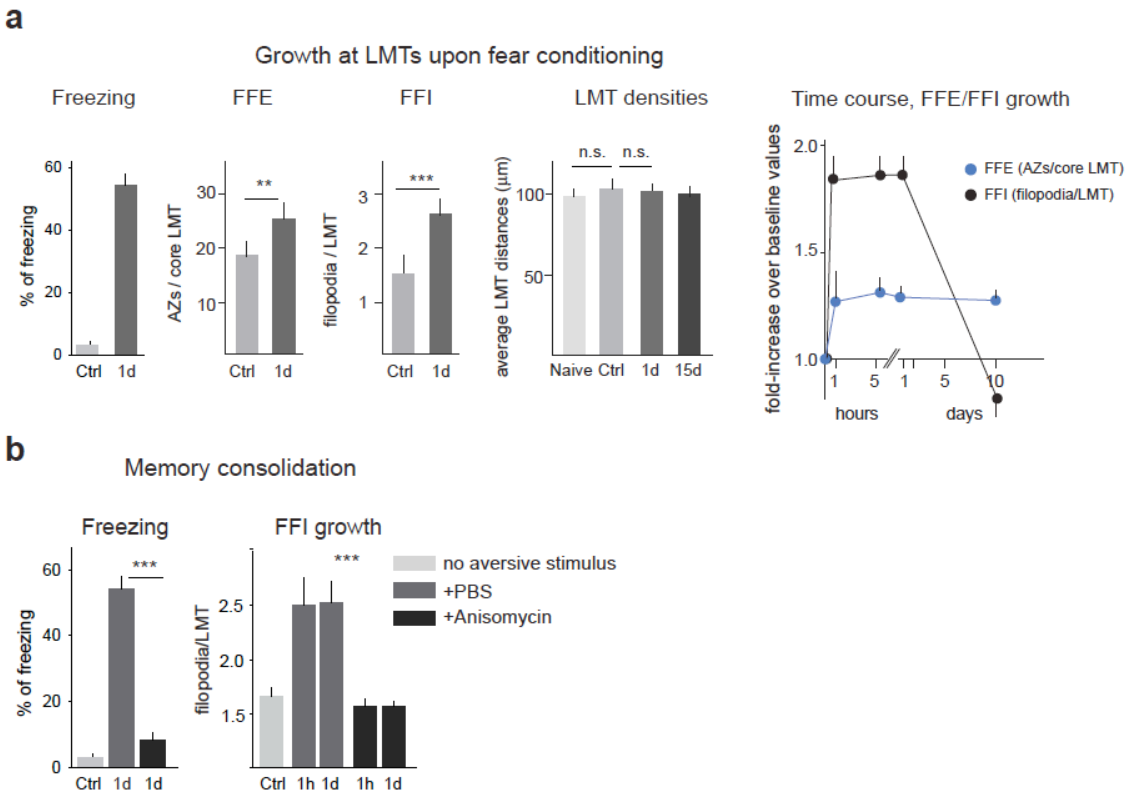

Supplementary Figure 2

Properties of feedforward inhibition connectivity growth upon contextual fear conditioning.

(**a**) Freezing: behavioral freezing upon fear conditioning, as shown in Fig. 3a. FFE and FFI: Extent of FFE (mean Bassoon puncta (i.e. AZs)/core LMT values) and FFI (mean filopodia/LMT values) growth 1d after fear conditioning. N=5, 50 LMTs each. LMT densities: average distance of LMTs (swellings with largest diameter > 3µm) along individual mGFP positive axons in CA3b; N=3, 30 LMT each. Naïve: cage control; Control: exposed to training context without aversive stimulus; 1d, 15d: time after fear conditioning. Time course of FFI and FFE growth upon fear conditioning: note how the more modest increase in FFE release sites persisted much longer than that in FFI connectivity. N=5 mice; 100 LMTs each.

(**b**) Protein synthesis blockade at learning prevents consolidation of fear memory and FFI growth. Anisomycin (75mg/kg body weight) or PBS were applied 20 min before, and 2h after (only for 1d time point) fear conditioning. N=5 mice, 100 LMTs each.

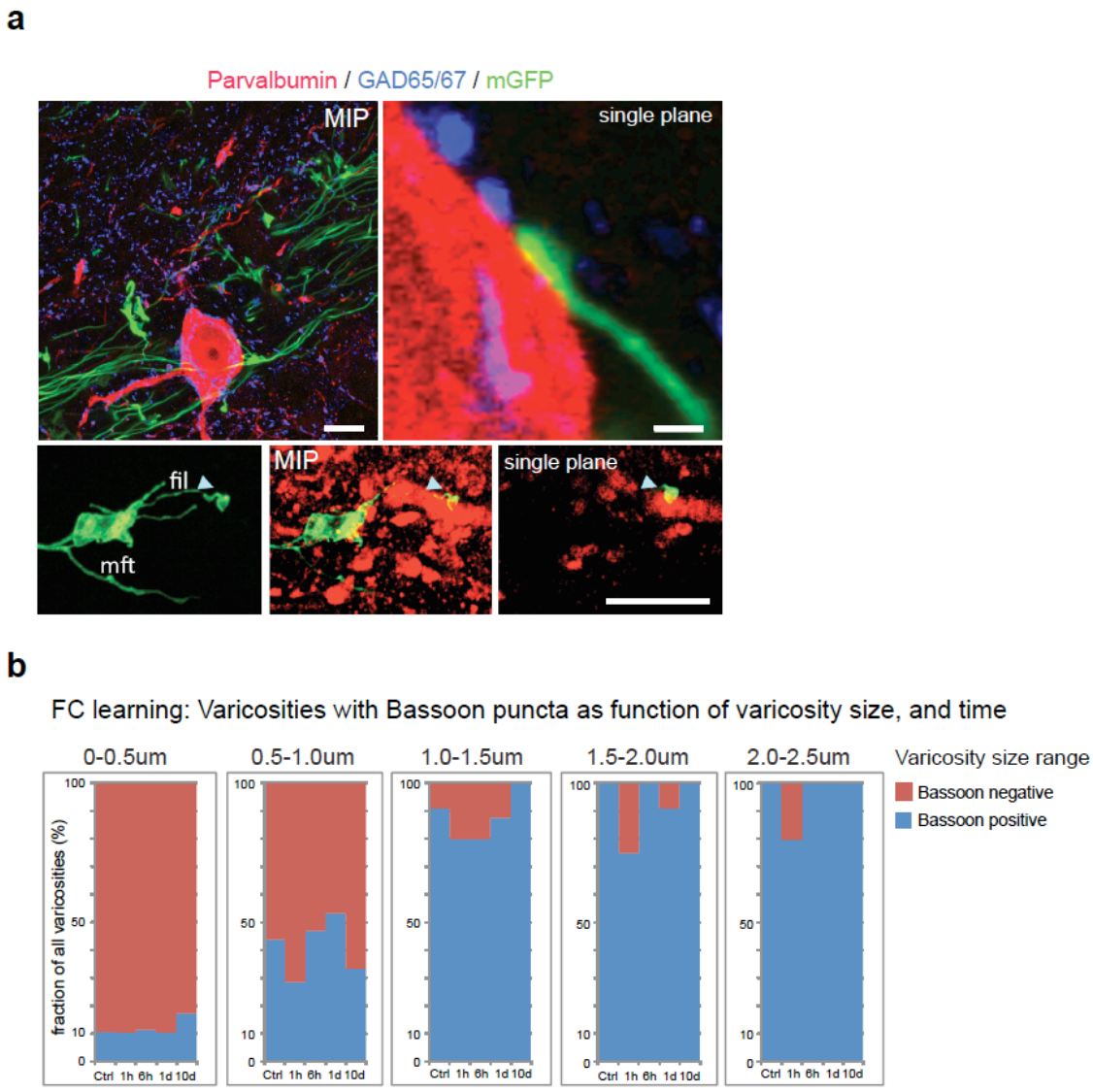

Supplementary Figure 3

Growth of FFI connectivity upon fear conditioning.

(**a**) LMT filopodia varicosities contact parvalbumin-positive interneurons in CA3. Examples of varicosities contacting soma (upper row) and dendrite (lower row, arrowheads) of parvalbumin-positive interneurons. MIP: maximum intensity projection; single plane: single confocal plane; fil: filopodium; mft: mossy fiber terminal. More than 95% of varicosities were in comparable contact with a parvalbumin-positive interneuron (N=600 varicosities, from 4 mice; not shown).

(**b**) Varicosities with Bassoon puncta as a function of varicosity size and time upon fear conditioning. N=3, 100 filopodia each. Note how most varicosities (filopodial swellings larger than 1 µm) exhibited Bassoon puncta, and how varicosities without Bassoon puncta were slightly more frequent at 1h and 6h after fear conditioning.

Bars: 10 and 0.5 (top row, right panel) µm.

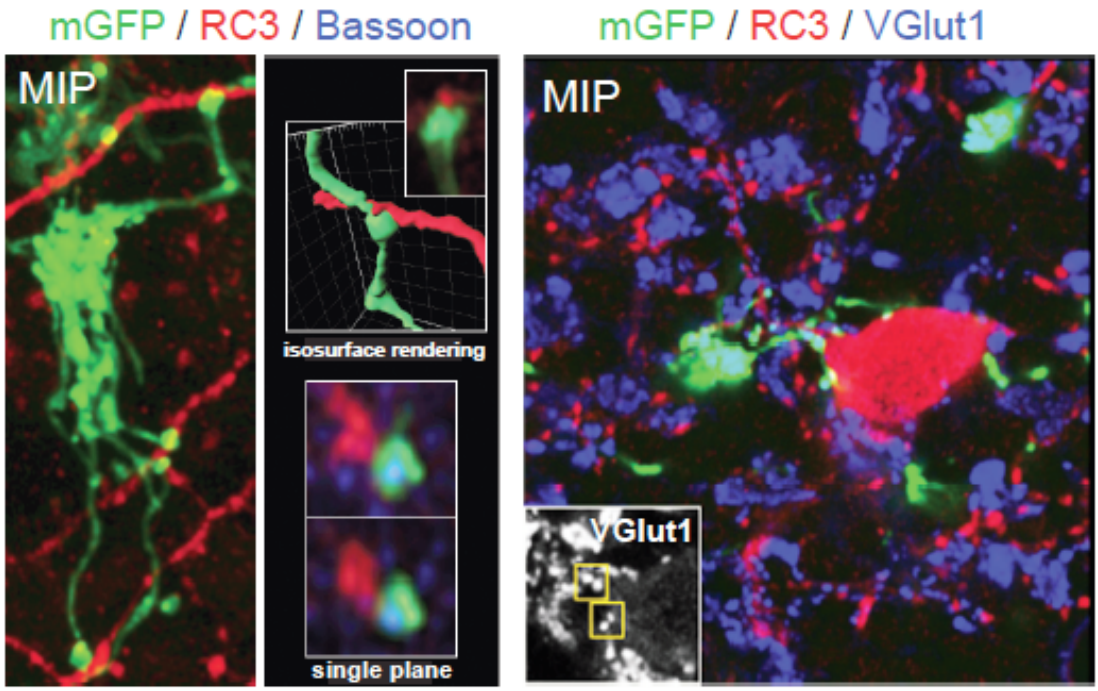

Supplementary Figure 4

Cerebellar mossy fiber terminal filopodia synapse onto Golgi cells. Examples of synaptic contacts onto RC3-positive Golgi cells are shown in the panels. Within granule cell layer volumes with an RC3-positive Golgi cell more than 95% of varicosities were in comparable contact with that RC3-positive Golgi cell (N=300 varicosities, from 3 mice). MIP: maximal intensity projection. VGlut1: vesicular glutamate transporter 1, which is expressed by cerebellar granule cells.

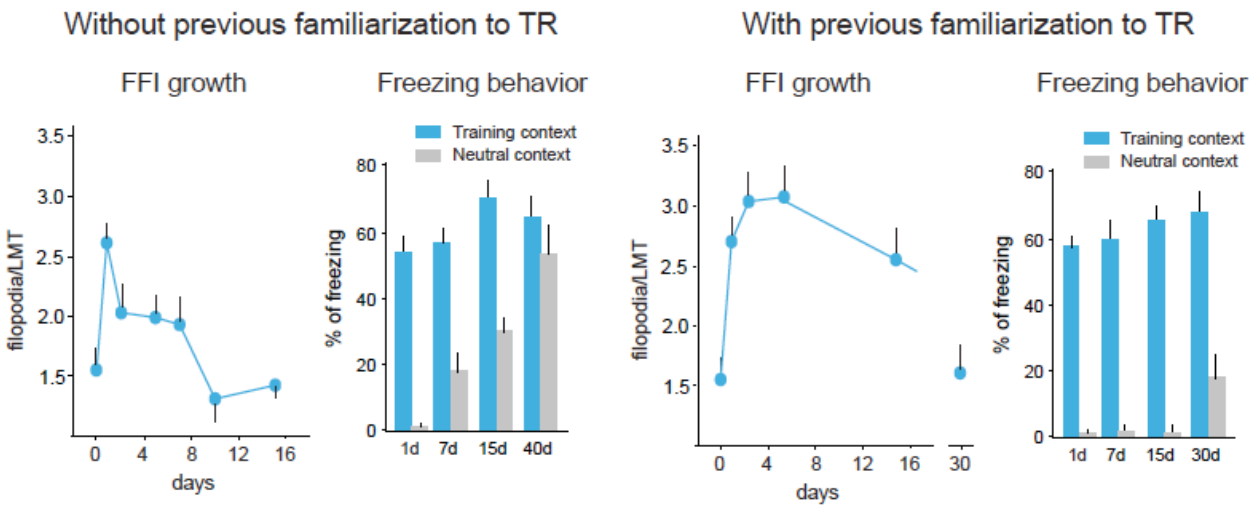

Supplementary Figure 5

Prolonged feedforward inhibition growth and delayed generalization upon previous familiarization with training context in contextual fear conditioning experiment. Experimental details as in Fig. 3c. N=5, 100 LMTs each.

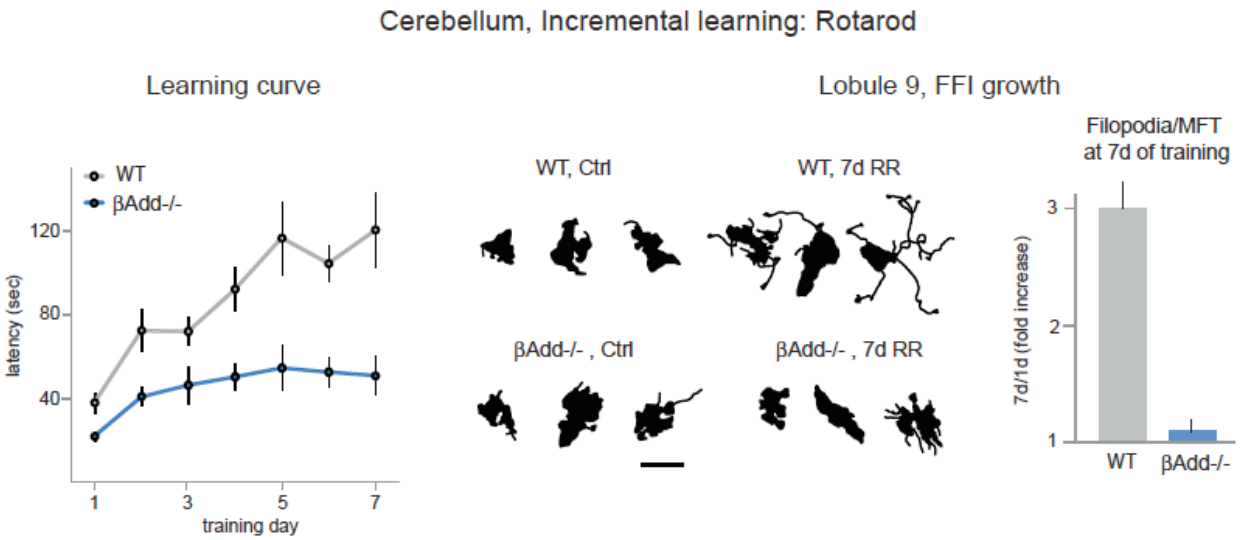

Supplementary Figure 6

Mice lacking β-Adducin have a major deficit in learning the rotarod task, and fail to establish extra filopodia in cerebellar cortex lobule 9 upon rotarod training. Experimental details as in Fig. 1f. N=3 mice, 100 LMT each. Bar: 10 μm.

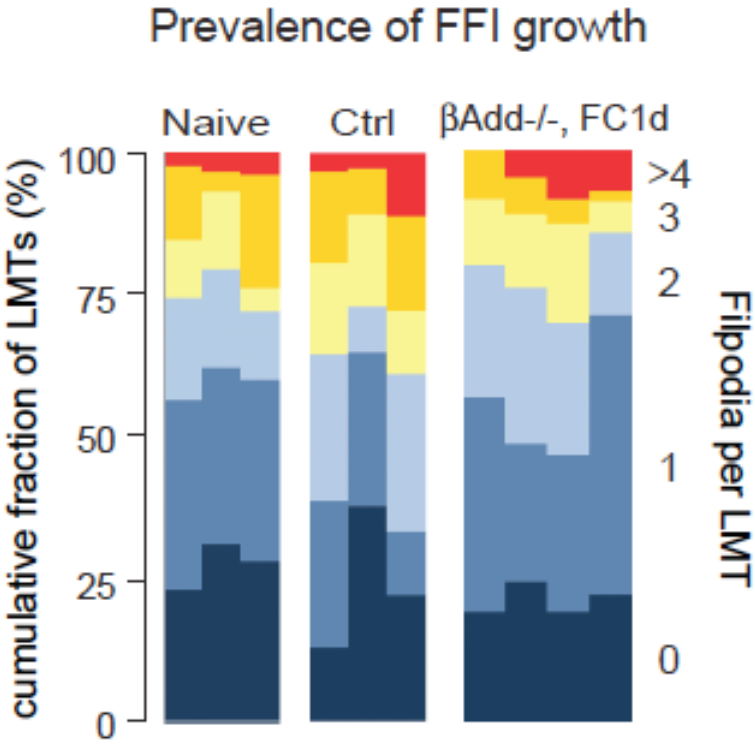

Supplementary Figure 7

Comparison of filopodia/LMT content distributions for individual wild-type (naïve; control, 1d) and *β-Adducin*$^{-/-}$ (FC, 1d) mice. N=100 LMTs. Details as in Fig. 1e.

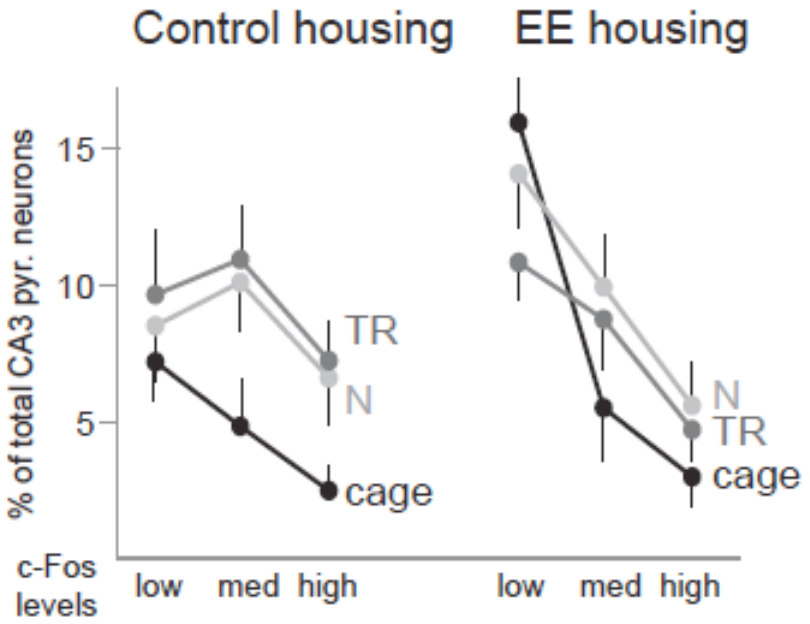

Supplementary Figure 8

Elevated recruitment of c-Fos in CA3 pyramidal neurons of mice housed under environmental enrichment (EE) conditions. Experimental conditions as in Fig. 4a. N=3, 400 pyramidal neurons each. EE housing was for 4 weeks. Control values are reproduced from Fig. 4a.